Steel and Composite Structures, *Vol. 19, No. 4 (2015) 967-993*
DOI: http://dx.doi.org/10.12989/scs.2015.19.4.967

Predicting the axial load capacity of high-strength concrete filled steel tubular columns

Farhad Aslani *1, Brian Uy [1a], Zhong Tao [2b] and Fidelis Mashiri [2c]

[1] *Centre for Infrastructure Engineering and Safety, The University of New South Wales, Sydney NSW 2052, Australia*
[2] *Institute for Infrastructure Engineering, Western Sydney University, Penrith NSW 2751, Australia*

(*Received October 31, 2014, Revised March 11, 2015, Accepted May 21, 2015*)

Abstract. The aim of this paper is to investigate the appropriateness of current codes of practice for predicting the axial load capacity of high-strength Concrete Filled Steel Tubular Columns (CFSTCs). Australian/New Zealand standards and other international codes of practice for composite bridges and buildings are currently being revised and will allow for the use of high-strength CFSTCs. It is therefore important to assess and modify the suitability of the section and ultimate buckling capacities models. For this purpose, available experimental results on high-strength composite columns have been assessed. The collected experimental results are compared with eight current codes of practice for rectangular CFSTCs and seven current codes of practice for circular CFSTCs. Furthermore, based on the statistical studies carried out, simplified relationships are developed to predict the section and ultimate buckling capacities of normal and high-strength short and slender rectangular and circular CFSTCs subjected to concentric loading.

Keywords: composite structures; concrete filled steel tubular columns; high-strength; axial load capacity

1. Introduction

Concrete Filled Steel Tubular Columns (CFSTCs) are finding increasing use in modern construction practice throughout the world. This increase in use is largely due to the structural and economical advantages offered by concrete filled tubes over hollow sections, as well as their aesthetic appeal. From a structural perspective, hollow sections exhibit high torsional and compressive resistance about both principal axes when compared with open sections. Additionally, the exposed surface area of a closed section is approximately two-thirds that of a similar sized open section, thus demanding reduced painting and fireproofing costs, (Packer and Henderson 2003). Composite columns comprise a combination of concrete and steel and utilise the most favourable properties of the constituent materials. Use of composite columns can result in

∗Corresponding author, Research Fellow, Ph.D., E-mail: f.aslani@unsw.edu.au
[a] Professor, Ph.D., E-mail: b.uy@unsw.edu.au
[b] Professor, Ph.D., E-mail: z.tao@westernsydney.edu.au
[c] Associate Professor, Ph.D., E-mail: f.mashiri@westernsydney.edu.au

http://www.techno-press.org/?journal=scs&subpage=8 ISSN: 1229-9367 (Print), 1598-6233 (Online)

significant savings in column size, which ultimately can lead to considerable economic savings. This reduction in column size is particularly beneficial where floor space is at a premium, such as in car parks and office blocks (Lam and Gardner 2008). The performance of CFSTCs can be further improved if high-strength materials are used. High-strength steel and concrete are found to be attractive alternatives to the normal-strength steel and concrete for multi-storey and high-rise construction.

Uy *et al*. (2013) reported that the use of various high-strength materials is currently limited by international codes of practice and further research is required to inform and update these standards. The American Institute of Steel Construction limits the maximum yield stress of steel to 525 MPa and the compressive strengths of concrete to 70 N/mm^2 (American Institute of Steel Construction 2010). The Eurocode 4 document limits the maximum yield stress of steel to 460 N/mm^2 and compressive strengths of concrete to 60 N/mm^2 (Eurocode 4 2004). The Chinese Standards also limit the maximum yield stress of steel to 420 N/mm^2 and compressive strength to 80 N/mm^2 (National Standard of the People's Republic of China 2002, 2003).

Recent advances in Australia now allow characteristic concrete cylinder compressive strengths up to 100 N/mm^2 (Standards Australia 2009) and recent revisions have incorporated the introduction of the use of high-strength steel up to nominal 690 N/mm^2 yield stress (Standards Australia 2012). This is in line with the internationally leading Hong Kong Steel Code which has also recently introduced the use of high-strength steel up to 690 N/mm^2 (Hong Kong Buildings Department 2005). The Australian/New Zealand standards for composite bridges and buildings are currently being revised and will also allow for the use of concrete filled steel columns with a concrete compressive strength of 100 N/mm^2 and steel yield strength of 690 N/mm^2, respectively (Standards Australia 2014a, b).

Consequently, considerable attention in current design guidelines has been directed in recent years towards investigating the performance of composite columns with different ranges of strengths of steel and concrete. There has been a move towards improving numerical methods for high-strength composite columns, which have controlled accuracy in contrast to expensive experimental tests or oversimplified analytical estimations. Furthermore, the complete behaviour of these members cannot be predicted accurately by available codes. Therefore, an accurate and simple numerical model is required in this case.

The aim of this study is to investigate the suitability of current codes of practice and models for predicting the section and ultimate buckling capacities of high-strength CFSTCs. Australian/New Zealand standards and other international codes of practice for composite bridges and buildings are currently being revised and will allow for the use of high-strength CFSTCs. Thus, it is important to check and modify the suitability of predicting the section and ultimate buckling capacities models.

For this purpose, many researchers have carried out short and slender composite column tests which have included: (a) rectangular and circular normal-strength steel tube columns filled with high-strength concrete (R&C-NSS-TC-HSC); (b) rectangular and circular high-strength steel tube columns filled with normal-strength concrete (R&C-HSS-TC-NSC); and (c) rectangular and circular high-strength steel tube columns filled with high-strength concrete (R&C-HSS-TC-HSC). Also, these experimental results are compared with the available axial load capacity numerical methods. Moreover, this research provides useful information for a future possible revision of current design guidelines. In this paper high-strength steel is considered for steel tubes with $f_y \geq$ 450 MPa and high strength concrete with $f'_c \geq 60$ MPa.

The effects of different parameters such as steel strength, concrete strength, and section slenderness on the accuracy of the strength predictions are discussed. Furthermore, in this paper simplified relationships are developed to predict the section and ultimate buckling capacities of normal and high-strength rectangular and circular CFSTCs subject to concentric loading.

2. Past research

Previous published research is categorized under the following three topics: (a) Normal-strength steel tube columns filled with high-strength concrete (NSS-TC-HSC); (b) High-strength steel tube columns filled with normal-strength concrete (HSS-TC-NSC); and (c) High-strength steel tube columns filled with high-strength concrete (HSS-TC-HSC).

2.1 Normal-strength steel tube columns filled with high-strength concrete (NSS-TC-HSC)

There are limited experimental studies on high-strength CFSTCs, such as those carried out by Rangan and Joyce (1992), Kilpatrick and Rangan (1999a, b), and Johansson (Johansson *et al*. 2001, Johansson 2002). For the static flexural behaviour, Varma *et al*. (2002a) investigated eight 110 N/mm^2 ultra-high-strength concrete (UHSC) filled square steel tubes subjected to axial load and monotonically increasing flexural loading. For seismic behaviour, Varma *et al*. (2002b, 2004) conducted a series of tests on the seismic behaviour of HSC filled square beam columns subjected to constant axial load and cyclically varying flexural loading. The cylinder strengths of the HSC were as high as 110 N/mm^2. Gho and Liu (2004) studied the flexural behaviour of twelve concrete filled rectangular steel hollow section specimens infilled with HSC of cylinder strengths varying between 56 and 91 N/mm^2. Melcher and Karmazinova (2004) also presented the test results of CFSTCs with high-strength concrete class between C55/67 and C80/95. Sakino *et al*. (2004) studied twenty HSC specimens with concrete strength between 77 and 91 N/mm^2 to investigate the behaviour of centrally loaded short CFSTCs. Han *et al*. (2008) tested fifty circular and square hollow structural steel stub columns infilled with self-compacting concrete of cube strengths between 50 and 90 N/mm^2.

For the combined concentrically and eccentrically loaded behaviour, Liu (2004, 2005, 2006) performed a series of tests on HSC filled rectangular steel tubular columns subjected to concentric and eccentric loading. The cylinder strengths of the HSC were about 60 and 90 N/mm^2. Yu *et al*. (2008) carried out an investigation on twenty eight thin-walled hollow square and circular steel tubes infilled with self-consolidating concrete with cube strength of 122 N/mm^2. De Oliveria *et al*. (2009) also reached conclusions on circular slender CFSTCs. The combination of D/t and steel strength in some of their tests was unable to provide sufficient confinement for the high-strength concrete core. Portolés *et al*. (2011) concluded that it was obvious that the use of HSC in slender concrete-filled tubular columns does not provide the same enhancement as that of NSC in composite members. In addition, Hernández-Figueirido *et al*. (2012) described thirty six experimental tests conducted on rectangular CFSTCs filled with concrete up to 90 N/mm^2 and subjected to axial compression and different eccentricities at both ends. The tests illustrated that the use of high-strength concrete is more beneficial for the cases of non-constant bending moment since second order effects are reduced. However, when the aim is to obtain ductile behaviour, the use of NSC is more suitable.

In view of recent progress into the use of UHSC with compressive strengths up to 200 N/mm^2 (Liew *et al*. 2008), Liew and Xiong (2010) presented an experimental investigation on sixteen axially loaded circular specimens including two hollow tubes, six filled tubes and eight filled double-tubes, involving UHSC. Steel fibres were added into the UHSC to study their effect in improving the ductility and strengths of composite columns. The ultimate resistance, residual plastic resistance and ductility were evaluated. Also, Liew and Xiong (2012) presented a very interesting experimental investigation on the performance of twenty seven axially loaded column specimens, including eighteen steel tubes infilled with UHSC of compressive strength close to 200 N/mm^2, four steel tubes infilled with NSC and five hollow steel tubes. Steel fibres were added into the UHSC to study their effect in improving the ductility and strength. However, these tests concentrated on stub columns and the UHSC was a commercial pre-blended mix mortar material.

2.2 High-strength steel tube columns filled with normal-strength concrete (HSS-TC-NSC)

Uy (1999) and Uy (2001a) presented the results of steel and composite sections fabricated using high-strength structural steel of nominal yield stress 690 N/mm^2 and NSC of 20 N/mm^2. These sections were constructed as stubby columns and were subjected to concentric axial compression. Uy (2001b) conducted an extensive experimental programme on short concrete filled steel box columns, which incorporated high-strength structural steel of Grade 690 N/mm^2. The experiments were then used to calibrate a refined cross-sectional analysis method, which considered both the non-linear material properties of the steel and concrete coupled with the measured residual stress distributions in the steel. Uy *et al*. (2002) conducted further research on high-strength steel box columns filled with concrete. This study consisted of three short columns and three slender columns to consider both the strength and stability aspects of steel-concrete composite high-strength composite columns.

Sakino *et al*. (2004) studied sixteen specimens with steel yield strengths between 507 and 853 N/mm^2 to investigate the behaviour of centrally loaded short CFSTCs, and proposed formulae to estimate the ultimate axial compressive capacities of CFSTCs. Mursi and Uy (2004, 2006a, b) carried out further experimental work on high-strength steel slender columns loaded uniaxially and biaxially and assessed the applicability of existing codes of practice to deal with high-strength steel and NSC. Their findings showed that existing codes of practice were quite conservative in dealing with these structural forms for biaxial loading in particular. Liew and Xiong (2010) also recently conducted a very comprehensive study on UHSC up to 200 N/mm^2 compressive strength of concrete with steel tubes of yield strength of about 450 N/mm^2. Aslani *et al*. (2015) presented the results of sixteen steel and composite sections fabricated using high-strength structural steel of nominal yield stress 701 N/mm^2 and concrete of 21-55 N/mm^2.

2.3 High-strength steel tube columns filled with high-strength concrete (HSS-TC-HSC)

Fujimoto *et al*. (1995) reported an extensive set of tests on square CFST stub columns subjected to combined compression and bending. A total of twenty two specimens with steel yield stresses of 260 to 835 N/mm^2 and concrete cylinder strengths varying from 25 to 80 N/mm^2 were tested. Test results showed that the strength of the CFST beam-columns was considerably affected by the B/t ratio and the axial load level. In addition, the specimens containing high-strength steel exhibited lower ductility than those fabricated from normal-strength steel.

Varma *et al*. (2002a, b) concluded from the tests on eight square CFST beam-columns that the moment capacity of the columns could be well predicted using the ACI provisions. The test specimens had a uniform concrete cylinder strength of 110 N/mm^2 and steel yield stresses ranging from 269 to 660 N/mm^2. Liu *et al*. (2003) studied twenty two CFST rectangular stub columns (f_y = 550 N/mm^2, and f'_c = 70-82 N/mm^2) subjected to concentric loading. Sakino *et al*. (2004) studied 15 specimens with concrete strength between 77 and 91 N/mm^2 and steel yield strength between 507 and 853 N/mm^2 to investigate the behaviour of centrally loaded short CFSTCS. Liu (2004, 2005, 2006) performed a series of tests on high-strength CFSTCS with concrete strength between 60 and 90 N/mm^2 and with steel yield strength between 495 and 550 N/mm^2.

Liew *et al*. (2008) presented an experimental investigation on the behaviour of UHSC filled square tubular columns exposed to axial loading. The cylinder strength of UHSC was up to 160 N/mm^2, and the yield strength of the steel plates for the welded square box sections was 780 N/mm^2. The load-deformation behaviour was recorded during the tests, and the cross-sectional maximum resistances were obtained, and their failure modes observed and reported.

Recently, Uy *et al*. (2013) presented an experimental investigation on CFSTCs with nominal yield strength of the steel sections of the columns as 690 N/mm^2, and the unconfined compressive strength of the inner concrete section of the CFSTCs with a range from 80 to 100 N/mm^2. Forty short specimens, with a length to width ratio of 3.5 and a width to thickness ratio of 15 to 40 were subjected to monotonic loading to investigate the ultimate strength, the local buckling effects and the confinement effects of the high-strength CFSTCs.

3. Experimental database

As outlined in section 2, the experimental results collected are categorised into three sub sections as follows: (a) Normal-strength steel tube columns filled with high-strength concrete (NSS-TC-HSC), (b) High-strength steel tube columns filled with normal-strength concrete (HSS-TC-NSC), and (c) High-strength steel tube columns filled with high-strength concrete (HSS-TC-HSC). Furthermore, this database is subdivided into columns of “circular, C” and “rectangular, R” (mainly square) cross-section and into “short” (defined as L/D or $L/B \leq 4$) and “slender” (L/D or $L/B > 4$) categories. The information required and reported for each test is: the outer diameter (D) of circular cross-section, width (B) and depth (D) of rectangular cross-section, the thickness of the steel tube (t), length of the column (L), yield strength of the steel tube (f_y), modulus of elasticity of the steel tube (E_s), compressive strength of the concrete (f'_c), modulus of elasticity of concrete (E_c), the maximum load achieved by the column in the test (N_{ue}).

If E_s was not provided in the study it was assumed to be 200 × 10^3 N/mm^2. Furthermore, E_c value was not provided it was calculated using the expression “3320 $(f'_c)^{0.5}$ + 6900” N/mm^2 where f'_c is given in N/mm^2 which was suggested by ACI (2008). Also, because the compressive strength of concrete test types of specimens in the database was varied, the f'_c values were corrected. In this study, compressive strength of concrete cylinder specimens with 150 × 300 mm dimension were considered as the default and the other types of specimens are converted by using conversion factors proposed by Yi *et al*. (2006). The concrete strength conversion factors are between cylinder specimens with 100 × 200 mm and 150 × 300 mm dimensions, cube specimens with 100 mm and 150 mm dimensions, and prism specimens with 150 × 150 × 300 mm dimension. Yi *et al*. (2006) proposed the conversion factors for high- and normal-strength concrete as shown in Table 1. The range of the test properties is provided in Table 2. The number of rectangular CFSTCs experimental tests that were included in the database was 306. Also, the number of circular CFSTCs experimental tests that were included in the database was 191.

4. Design code models

In the past, many researchers and design guidelines proposed empirical models for the prediction of the section and ultimate buckling capacities of CFSTCs. Different models and design philosophies have been adopted in design codes. The practical application of CFST construction is now supported by codes and recommendations, such as the Japanese code AIJ (1997), American code AISC (American Institute of Steel Construction 2005), Chinese code DBJ 13-51-2003 (2003), Eurocode 4 (2004), AS5100.6 (2004), etc.

Table 1 Compressive concrete strength conversion factors

For high strength concrete	$f'_{cy(150\times300)}$	$f'_{cu(100)}$	$f'_{cu(150)}$	$f'_{c,pr(150)}$
$f'_{cy(100\times200)}$	1.04	0.96	1.02	1.11
$f'_{cy(150\times300)}$	1.00	0.92	0.98	0.94
For normal strength concrete	$f'_{cy(150\times300)}$	$f'_{cu(100)}$	$f'_{cu(150)}$	$f'_{c,pr(150)}$
$f'_{cy(100\times200)}$	1.03	0.85	0.91	1.07
$f'_{cy(150\times300)}$	1.00	0.82	0.88	1.05

Table 2 Experimental results database properties

Properties range	Rectangular columns type		
	NSS-TC-HSC	HSS-TC-NSC	HSS-TC-HSC
D or *B* (mm)	60-324	110-300	75-319
D/*t* or *B*/*t*	20-107	14-52	15-53
λ_e (plate element slenderness)	23-117	19-93	27-89
f'_c (N/mm^2)	60-130	20-60	55-110
f_y (N/mm^2)	250-450	450-850	450-850
Short columns (%)	65	75	80
Long columns (%)	35	25	20
No. of tests	143	67	96
No. of references	12	8	10
Properties range	Circular columns type		
	NSS-TC-HSC	HSS-TC-NSC	HSS-TC-HSC
D or *B* (mm)	60-450	108-360	108-360
D/*t* or *B*/*t*	19-220	14-80	16-80
λ_e	21-215	35-195	51-195
f'_c (N/mm^2)	60-115	20-50	55-85
f_y (N/mm^2)	185-450	450-855	500-850
Short columns (%)	72	80	86
Long columns (%)	28	20	14
No. of tests	120	57	14
No. of references	12	7	4

Research and practice of CFST members and structures has also led to the development of these design codes. The collected design codes and models for prediction of axial capacity are categorised in two subdivisions into “circular, C” and “rectangular, R” similar to the experimental results database. In the collected database the following models are included for the rectangular CFSTCs: Chinese code GJB 4142 (2001), Japanese code AIJ (2001), AS (AS4100 2012, AS3600 2001), Chinese code DBJ 13-51 (2003), Eurocode 4 (2004), AS5100.6 (2004), ACI (2005), and AISC (2005). Moreover, for circular CFSTCS the following models are included: CECS 28:90 (1992), AIJ (2001), and AS (AS4100 2012, AS3600 2001), Eurocode 4 (2004), AS5100.6 (2004), ACI (2005), and AISC (2005). Different limitations are prescribed in the available codes and models. These limitations and main models for rectangular and circular CFSTCs are summarised and presented in Tables 3 and 4. The presented models in Tables 3 and 4 are applicable for section capacity or ultimate buckling capacity of CFST members.

Table 3 Axial load capacity models for rectangular CFSTCs

Ref.	Rectangular CFSTCs	Type
GJB 4142 (2000)	$N_u = A_{sc} f_{sc}$ $f_{sc} = \left(1.212 + \alpha\,\xi + \beta\,\xi^2\right) f_{ck}$ $\alpha = 0.1381 \times \left(f_y / 215\right) + 0.7646$ $\beta = -0.0727 \times \left(f_{ck} / 15\right) + 0.0216$ $\xi = A_s f_y / A_c f_{ck}$ $f_{ck} = 0.67\, f'_{cu} = 0.80\, f'_{cy}$	Section capacity
AIJ (2001)	$N_{u1} = N_{cu,c} + \left(1+\eta\right) N_{cu,s} \quad l/D \le 4$ $N_{u2} = N_{u1} - 0.125\left\{N_{u1} - N_{u3}\left(l/D - 12\right)\right\}\left(l/D - 4\right) \quad 4 < l/D \le 12$ $N_{u3} = N_{cr,c} + N_{cr,s} \quad l/D > 12$ $N_{cu,c} = A_c\, r_{u,c}\, f'_c$ $N_{cr,c} = A_c\, \sigma_{cr}$ $\sigma_{cr} = \dfrac{2}{1 + \sqrt{\lambda_1^4 + 1}}\, r_{u,c}\, f'_c \qquad \lambda_1 \le 1.0$ $\sigma_{cr} = 0.83\, exp\left\{C_c\left(1 - \lambda_1\right)\right\}\, r_{u,c}\, f'_c \qquad \lambda_1 > 1.0$ $\lambda_1 = \dfrac{\lambda}{\pi}\sqrt{\varepsilon_{u,c}}$ $\varepsilon_{u,c} = 0.93\left(r_{u,c}\, f'_c\right)^{1/4} \times 10^{-3}$ $C_c = 0.568 + 0.00612\, f'_c$ $N_{cu,s} = A_s\, f_y$ $N_{cr,s} = \begin{Bmatrix} A_s\, f_y & \lambda_1 < 0.3 \\ 1 - 0.545\left(\lambda_1 - 0.3\right) & 0.3 \le \lambda_1 < 1.3 \\ N_{E,s}/1.3 & \lambda_1 \ge 1.3 \end{Bmatrix}$ $\lambda_1 = \dfrac{\lambda}{\pi}\sqrt{\dfrac{f_y}{E_s}}$	Ultimate buckling capacity

Table 3 Continued

Ref.	Rectangular CFSTCs	Type
AIJ (2001)	$N_{E,s} = \frac{\pi^2 E_s I_s}{l^2}$ $\frac{B}{t} \leq 1.5 \frac{735}{\sqrt{f_y}}$ l : effective length of a CFT column, D : width or diameter of a steel tube section η = 0 for a square CFT column $r_{u,c}$= 0.85: reduction factor for concrete strength λ: slenderness ratio of a concrete column	Ultimate buckling capacity
DBJ 13-51 (2003)	$N_u = A_{sc} f_{sc}$ $f_{sc} = (1.14 + 1.02\,\xi_0) f_{ck}$ $\xi = A_s f_y / A_c f_{ck}$ $f_{ck} = 0.67\, f'_{cu} = 0.80\, f'_{cy}$	Section capacity
Eurocode 4 (2004)	$N_u = A_s f_y + 0.85\, A_c f'_c$ $\frac{B}{t} \leq 52 \sqrt{\frac{235}{f_y}}$	Section capacity
AS5100.6 (2004)	$N_{uc} = \alpha_c \left(A_s\, f_y + A_c f'_c\right) \leq N_{us}$ $\alpha_c = \xi \left[1 - \sqrt{1 - \left(\frac{90}{\xi\,\lambda}\right)^2}\right]$ $\xi = \frac{\left(\frac{\lambda}{90}\right)^2 + 1 + \eta}{2\left(\frac{\lambda}{90}\right)^2}$ $\lambda = \lambda_\eta + \alpha_a\, \alpha_b$ $\eta = 0.00326\, \left(\lambda_\eta - 13.5\right) \geq 0$ $\lambda_\eta = 90\,\lambda_r$ $\alpha_a = \frac{2100\left(\lambda_\eta - 13.5\right)}{\lambda_\eta^2 - 15.3\,\lambda_\eta + 2050}$ α_b presented in the code. $\lambda_r = \sqrt{\frac{N_s}{N_{cr}}}$ $N_s = A_s\, f_y + A_c f'_c$ $N_{cr} = \frac{\pi^2 \left(EI\right)_{eff}}{l^2}$ $\left(EI\right)_{eff} = E_s\, I_s + E_c\, I_c$	Ultimate buckling capacity

Table 3 Continued

Ref.	Rectangular CFSTCs	Type
AS (AS4100 2012, AS3600 2001) and ACI (2005)	$N_u = A_s\ f_y + 0.85\ A_c\ f'_c$ $\frac{B}{t} \le \sqrt{\frac{3\ E_s}{f_y}}$	Section capacity
AISC (2005)	$N_u = 0.75\ N_n$ $N_n = \begin{cases} N_o\left[0.658^{(N_o/N_e)}\right] & N_e \ge 0.44\,N_o \\ 0.877\,N_e & N_e < 0.44\,N_o \end{cases}$ $N_o = A_s\ f_y + 0.85\,A_c\ f'_c$ $N_e = \pi^2\left(EI_{eff}\right)/\left(KL\right)^2$ $EI_{eff} = E_s\ I_s + C_3\ E_c\ I_c$ $C_3 = 0.6 + 2\left(\frac{A_s}{A_c + A_s}\right) \le 0.9$ $A_s \ge 0.01 A_g$ $f_y \le 525\ MPa;\ \ 21 \le f'_c \le 70\ MPa;\ \ \frac{b}{t} \le \sqrt{\frac{3\ E_s}{f_y}}$	Ultimate buckling capacity

Table 4 Axial load capacity models for circular CFSTCs

Ref.	Circular CFSTCs	Type
CECS 28:90 (1992)	$N_u = \rho_l\ \rho_e\ N_0$ $N_0 = A_c\ f'_{c,pr}\ \left(1 + \sqrt{\xi} + \xi\right)$ $\xi = A_s f_y\ /\ A_c\ f'_{c,pr}$ The ρ_e and ρ_l are reduction factors consider the eccentric loading effect and slenderness influence, respectively. For concentric loading, $\rho_e = 1$, and $\rho_l = \begin{cases} 1 - 0.115\sqrt{l_e / D - 4} & l_e / D > 4 \\ 1 & l_e / D \le 4 \end{cases}$ where l_e is the effective length of the column, which is determined by the supporting conditions. $0.3 \le \xi < 3.0$; $15\sqrt{235 / f_s} \le D / t \le 85\sqrt{235 / f_s}$	Section capacity
AIJ (2001)	$N_{u1} = N_{cu,c} + \left(1 + \eta\right) N_{cu,s} \quad l / D \le 4$ $N_{u2} = N_{u1} - 0.125\left\{N_{u1} - N_{u3}\left(l / D = 12\right)\right\}\left(l / D - 4\right) \quad 4 < l / D \le 12$ $N_{u3} = N_{cr,c} + N_{cr,s} \quad l / D > 12$ $N_{cu,c} = A_c\ r_{u,c}\ f'_c$ $N_{cr,c} = A_c\ \sigma_{cr}$	Ultimate buckling capacity

Table 4 Continued

Ref.	Circular CFSTCs	Type
AIJ (2001)	$\sigma_{cr} = \frac{2}{1+\sqrt{\lambda_1^4+1}} r_{u,c}\, f'_c \qquad \lambda_1 \le 1.0$ $\sigma_{cr} = 0.83\, exp\{C_c\,(1-\lambda_1)\}\; r_{u,c}\, f'_c \qquad \lambda_1 > 1.0$ $\lambda_1 = \frac{\lambda}{\pi}\sqrt{\varepsilon_{u,c}}$ $\varepsilon_{u,c} = 0.93\,(r_{u,c}\, f'_c)^{1/4} \times 10^{-3}$ $C_c = 0.568 + 0.00612\, f'_c$ $N_{cu,s} = A_s\, f_y$ $N_{cr,s} = \begin{Bmatrix} A_s\, f_y & \lambda_1 < 0.3 \\ 1-0.545\,(\lambda_1 - 0.3) & 0.3 \le \lambda_1 < 1.3 \\ N_{E,s}/1.3 & \lambda_1 \ge 1.3 \end{Bmatrix}$ $\lambda_1 = \frac{\lambda}{\pi}\sqrt{\frac{f_y}{E_s}}$ $N_{E,s} = \frac{\pi^2\, E_s\, I_s}{l^2}$ $\frac{D}{t} \le 1.5\frac{23500}{f_y}$ l : effective length of a CFT column; D : width or diameter of a steel tube section η = 0.27 for a circular CFT column; $r_{u,c}$ = 0.85: reduction factor for concrete strength; λ: slenderness ratio of a concrete column	Ultimate buckling capacity
AS (AS4100 2012, AS3600 2001) and ACI (2005)	$N_u = A_s\, f_y + 0.85\, A_c\, f'_c$ $\frac{D}{t} \le \sqrt{\frac{8\, E_s}{f_y}}$	Section capacity
Eurocode 4 (2004)	$N_u = \eta_2\, A_s\, f_y + \left(1+\eta_1\,\frac{t}{D}\frac{f_y}{f'_c}\right) A_c f'_c$ $\eta_1 = 4.9 - 18.5\,\lambda + 17\,\lambda^2 \quad (\eta_1 \ge 0);\; \eta_2 = 0.25\,(3+2\,\lambda) \quad (\eta_2 \ge 0)$ $\eta_1 = 0.25\,(3+2\,\lambda) \quad (\eta_2 \ge 0)$ $N_{plR} = A_s\, f_y + A_c f'_c$ $N_{cr} = \frac{\pi^2\,(EI)_{eff}}{l^2}$ $(EI)_{eff} = E_s\, I_s + 0.6\, E_c\, I_c$ $E_c = 22000\,\sqrt[3]{f'_c/10}$ $E_s = 2.1 \times 10^5$ $f_y \le 460\; MPa\;;\; 20 \le f'_c \le 60\; MPa$ $(D/t) \le 90\;(235/f_y)$	Ultimate buckling capacity

Table 4 Continued

Ref.	Circular CFSTCs	Type
AS5100.6 (2004)	$N_u = \alpha_c \left(\eta_2 A_s f_y + \left(1 + \frac{\eta_1 t f_y}{d_o f'_c} \right) A_c f'_c \right)$ $\eta_1 = 4.9 - 18.5 \lambda_r + 17 \lambda_r^2 \quad (\eta_1 \geq 0)$ $\eta_2 = 0.25 (3 + 2 \lambda_r) \quad (\eta_2 \geq 0)$ $\alpha_c = \xi \left[1 - \sqrt{1 - \left(\frac{90}{\xi \lambda} \right)^2} \right]$ $\xi = \frac{\left(\frac{\lambda}{90} \right)^2 + 1 + \eta}{2 \left(\frac{\lambda}{90} \right)^2}$ $\lambda = \lambda_\eta + \alpha_a \alpha_b$ $\eta = 0.00326 (\lambda_\eta - 13.5) \geq 0$ $\lambda_\eta = 90 \lambda_r$ $\alpha_a = \frac{2100 (\lambda_\eta - 13.5)}{\lambda_\eta^2 - 15.3 \lambda_\eta + 2050}$ α_b presented in the code. $\lambda_r = \sqrt{\frac{N_s}{N_{cr}}}$ $N_s = A_s f_y + A_c f'_c$ $N_{cr} = \frac{\pi^2 (EI)_{eff}}{l^2}$ $(EI)_{eff} = E_s I_s + E_c I_c$	Ultimate buckling capacity
AISC (2005)	$N_u = 0.75 N_n$ $N_n = \begin{cases} N_o \left[0.658^{(N_o/N_e)} \right] & N_e \geq 0.44 N_o \\ 0.877 N_e & N_e < 0.44 N_o \end{cases}$ $N_o = A_s f_y + 0.95 f'_c$ $N_e = \pi^2 (EI_{eff}) / (KL)^2$ $EI_{eff} = E_s I_s + C_3 E_c I_c$ $C_3 = 0.6 + 2 \left(\frac{A_s}{A_c + A_s} \right) \leq 0.9$ $A_s \geq 0.01 A_g$ $f_y \leq 525\ MPa$ $21 \leq f'_c \leq 70\ MPa$ $\frac{D}{t} \leq \sqrt{\frac{8 E_s}{f_y}}$	Ultimate buckling capacity

5. Comparisons of experiments and models

When comparing design calculations with the tests, the material partial safety factors specified in all the design codes was set to unity. At the same time, all code limitations are ignored for the purposes of checking the feasibility of the design codes in predicting the load-carrying capacities of the test specimens. In the available codes, the prediction of ultimate capacity for CFSTCs follows two steps: (1) determination of section capacity; and (2) adopting a slenderness reduction factor to determine the overall buckling resistance of columns. Therefore, the comparison between experimental results and code prediction should also be divided into two parts, section capacity and ultimate buckling capacity of CFSTCs. In this paper, firstly, the section capacity model is modified through the comparison of short columns, and secondly, essential modification on the slenderness reduction factor based on the modified formula of section capacity is undertaken and then the test/prediction ratios for slender columns are compared.

In order to better reflect the deviations of code predictions from the experimental results, the –10% and +10% error bounds are provided in the figures presented in the following sub-sections. It is worth noting that this is not a criterion used to assess the acceptability of the prediction accuracy. Generally, a reliability analysis should be performed based on a regional reliability standard to accomplish this task (Han *et al*. 2008, Tao *et al*. 2008).

In the following sections 5.1 and 5.2 a plot of the short and slender rectangular and circular CFSTCs experimental results (N_{ue}) versus available section capacity and ultimate buckling capacity models (N_{uc}) and N_{ue}/N_{uc} ratios versus compressive strength of concrete (f'_c) and steel yielding strength (f_y) are presented.

5.1 Short CFSTCs

Table 5 shows comparisons of the N_{ue}/N_{uc} ratios for the short rectangular CFSTCs experimental results and available section capacity models in Table 3.

Table 5 shows that the "AS (AS4100 2012, AS3600 2001), ACI (2005), and Eurocode 4 (2004)" models provide a better prediction for the short rectangular CFSTCs with an average value of N_{ue}/N_{uc} ratio of 1.02 compared with the other available models. A new design relationship is developed on the basis of the above better selected models for rectangular CFSTCs and is illustrated as Eq. (1). Eq. (1) has the following limitations as: $250 \le f_y$ (N/m^2) ≤ 850 and $20 \le f'_c$ (N/mm^2) ≤ 130.

$$N_u = A_s f_y + 0.87 A_c f'_c \tag{1}$$

Fig. 1 shows plot of the N_{ue} versus N_{uc} for the proposed circular CFSTCs model. The proposed relationship for rectangular CFSTCs provides a better prediction with an average value and standard deviation of N_{ue}/N_{uc} ratio of 1.00 and 0.16.

Also, Table 5 shows that the "AS (AS4100 2012, AS3600 2001), ACI (2005)" models provide a better prediction for the short circular CFSTCs with an average value of N_{ue}/N_{uc} ratio of 1.11 compared with the other available model. A new design relationship is developed on the basis of the above better selected models for circular CFSTCs and is illustrated as Eq. (2). Eq. (2) has the following limitations as: $200 \le f_y$ (N/m^2) ≤ 860 and $20 \le f'_c$ (N/mm^2) ≤ 120.

$$N_u = A_s f_y + 0.82 A_c f'_c \tag{2}$$

Table 5 Comparison of results of available section capacity models and proposed relationship with test results for short rectangular and circular CFSTCs

	R-NSS-TC-HSC		R-HSS-TC-NSC		R-HSS-TC-HSC	
f'_c range	$60 \le f'_c$ (N/mm^2) ≤ 130		$20 \le f'_c$ (N/mm^2) ≤ 60		$60 \le f'_c$ (N/mm^2) ≤ 110	
f_y range	$250 \le f_y$ (N/mm^2) ≤ 450		$450 \le f_y$ (N/mm^2) ≤ 850		$450 \le f_y$ (N/mm^2) ≤ 850	
Ref.	N_{ue}/N_{uc}		N_{ue}/N_{uc}		N_{ue}/N_{uc}	
	$\bar{x}$ *	$\bar{\sigma}$ *	$\bar{x}$	$\bar{\sigma}$	$\bar{x}$	$\bar{\sigma}$
GJB 4142 (2000)	1.20	0.41	0.71	0.17	0.89	0.24
DBJ 13-51 (2003)	1.28	0.44	0.94	0.14	0.89	0.23
Eurocode 4 (2004)	1.07	0.21	1.05	0.17	0.94	0.25
AS (AS4100 2012, AS3600 2001) and ACI (2005)	1.07	0.21	1.05	0.17	0.94	0.25
Proposed relationship	$\bar{x}$	$\bar{\sigma}$	$\bar{x}$	$\bar{\sigma}$	$\bar{x}$	$\bar{\sigma}$
	1.00	0.12	0.99	0.15	1.03	0.16
	C-NSS-TC-HSC		C-HSS-TC-NSC		C-HSS-TC-HSC	
f'_c range	$60 \le f'_c$(N/mm^2) ≤ 115		$20 \le f'_c$(N/mm^2) ≤ 50		$60 \le f'_c$(N/mm^2) ≤ 85	
f_y range	$185 \le f_y$(N/mm^2) ≤ 450		$450 \le f_y$(N/mm^2) ≤ 855		$500 \le f_y$(N/mm^2) ≤ 850	
Ref.	N_{ue}/N_{uc}		N_{ue}/N_{uc}		N_{ue}/N_{uc}	
	$\bar{x}$	$\bar{\sigma}$	$\bar{x}$	$\bar{\sigma}$	$\bar{x}$	$\bar{\sigma}$
CECS 28:90 (1992)	0.90	0.13	0.85	0.15	0.81	0.04
AS (AS4100 2012, AS3600 2001) and ACI (2005)	1.11	0.15	1.12	0.16	1.10	0.16
Proposed relationship	$\bar{x}$	$\bar{\sigma}$	$\bar{x}$	$\bar{\sigma}$	$\bar{x}$	$\bar{\sigma}$
	1.05	0.22	1.03	0.18	1.04	0.19

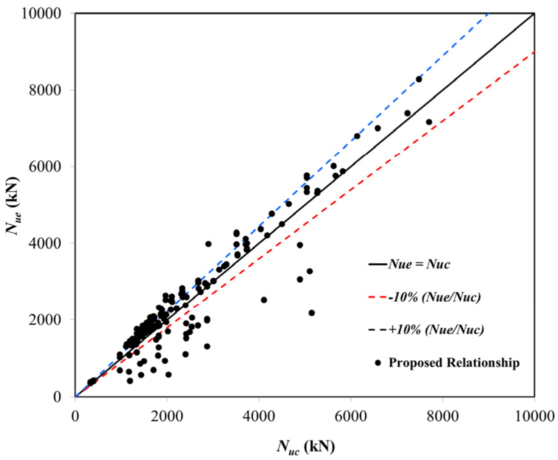

Fig. 1 Comparison of experimental results with predicted results by proposed section capacity relationship for short rectangular CFSTCs

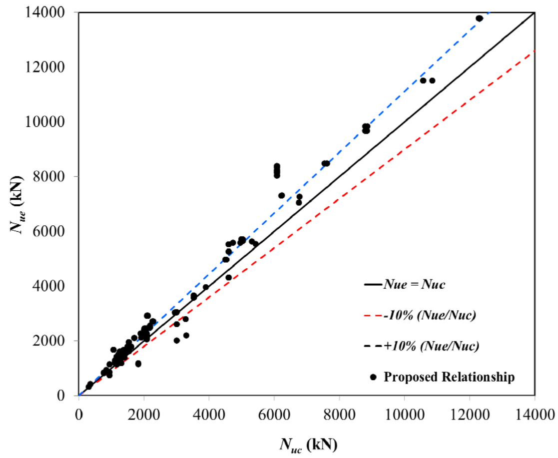

Fig. 2 Comparison of experimental results with predicted results by proposed section capacity relationship for short circular CFSTCs

Fig. 2 shows plot of the N_{ue} versus N_{uc} for the proposed circular CFSTCs model. The proposed relationship for circular CFSTCs provides a better prediction with an average value and standard deviation of N_{ue}/N_{uc} ratio of 1.05 and 0.14.

5.2 Slender CFSTCs

5.2.1 Rectangular slender CFSTCs

Table 6 shows comparisons of the N_{ue}/N_{uc} ratios for the slender rectangular CFSTCs experimental results and available section capacity models in Table 3.

Figs. 3 to 9 show plots of the experimental ultimate load, N_{ue} for the slender R-NSS-TC-HSC, R-HSS-TC-NSC, and R-HSS-TC-HSC results versus the calculated ultimate load, N_{uc} for the available models and N_{ue}/N_{uc} ratios versus f'_c. Table 6 shows that the "AS5100.6 (2004)" model provides a better prediction with an average value of N_{ue}/N_{uc} ratios of 0.93 compared with the other available models in Table 3 for the R-NSS-TC-HSC, R-HSS-TC-NSC, and R-HSS-TC-

Table 6 Comparison of results of available models and relationship with test results for slender rectangular CFSTCs

	R-NSS-TC-HSC		R-HSS-TC-NSC		R-HSS-TC-HSC	
f'_c range	$60 \leq f'_c$ (N/mm^2) ≤ 130		$20 \leq f'_c$ (N/mm^2) ≤ 60		$60 \leq f'_c$ (N/mm^2) ≤ 110	
f_y range	$250 \leq f_y$ (N/mm^2) ≤ 450		$450 \leq f_y$ (N/mm^2) ≤ 850		$450 \leq f_y$ (N/mm^2) ≤ 850	
Ref.	N_{ue}/N_{uc}		N_{ue}/N_{uc}		N_{ue}/N_{uc}	
	$\bar{x}$	$\bar{\sigma}$	$\bar{x}$	$\bar{\sigma}$	$\bar{x}$	$\bar{\sigma}$
AIJ (2001)	0.82	0.24	0.94	0.16	0.88	0.26
AS5100.6 (2004)	0.94	0.18	0.93	0.14	0.91	0.18
AISC (2005)	0.83	0.25	0.89	0.17	0.87	0.21
Proposed relationship		$\bar{x}$			$\bar{\sigma}$	
		0.97			0.14	

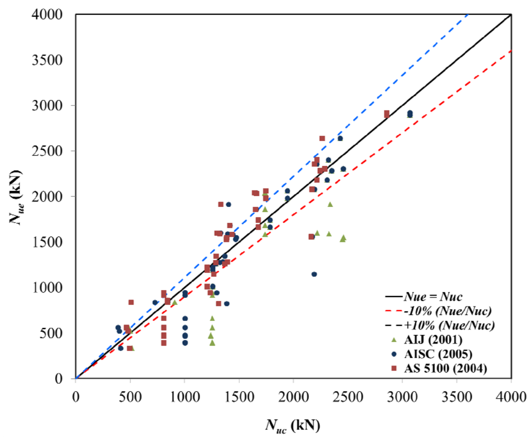

Fig. 3 Comparison of experimental results with predicted results by the existing models for slender R-NSS-TC-HSC

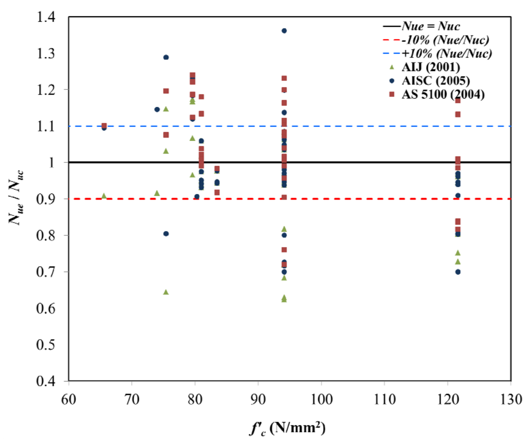

Fig. 4 Ratio experimental results/predicted results versus concrete strength for slender R-NSS-TC-HSC

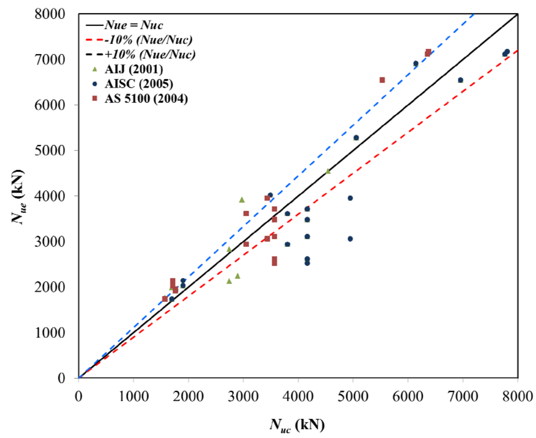

Fig. 5 Comparison of experimental results with predicted results by the existing models for slender R-HSS-TC-NSC

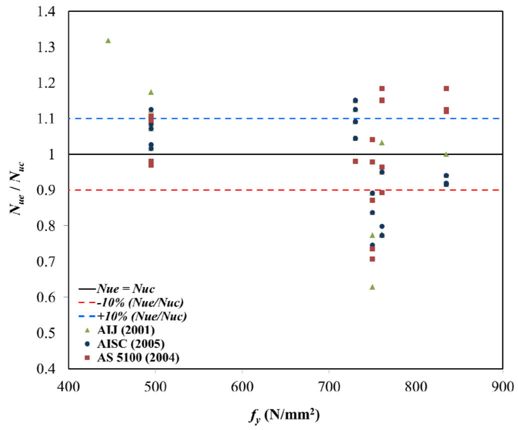

Fig. 6 Ratio experimental results/predicted results versus steel yielding strength for slender R-HSS-TC-NSC

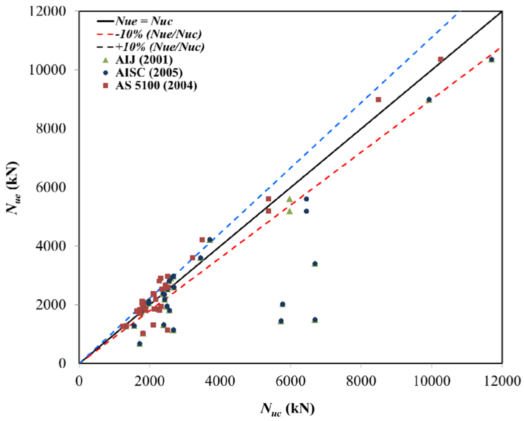

Fig. 7 Comparison of experimental results with predicted results by the existing models slender for R-HSS-TC-HSC

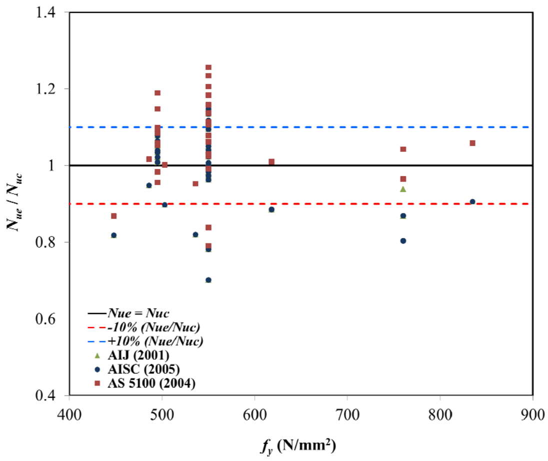

Fig. 8 Ratio experimental results/predicted results versus steel yielding strength for slender R-HSS-TC-HSC

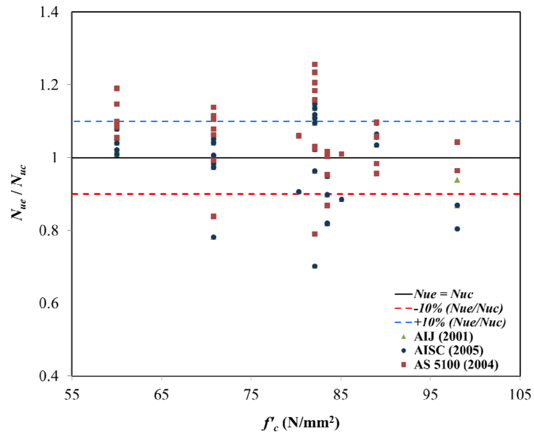

Fig. 9 Ratio experimental results/predicted results versus concrete strength for slender R-HSS-TC-HSC

Table 7 Comparison of results of available models and relationship with test results for slender circular CFSTCs

	C-NSS-TC-HSC		C-HSS-TC-NSC		C-HSS-TC-HSC	
f'_c range	$60 \leq f'_c$ (N/mm^2) ≤ 115		$20 \leq f'_c$ (N/mm^2) ≤ 50		$60 \leq f'_c$ (N/mm^2) ≤ 85	
f_y range	$185 \leq f_y$ (N/mm^2) ≤ 450		$450 \leq f_y$ (N/mm^2) ≤ 855		$500 \leq f_y$ (N/mm^2) ≤ 850	
Ref.	N_{ue}/N_{uc}		N_{ue}/N_{uc}		N_{ue}/N_{uc}	
	$\bar{x}$	$\bar{\sigma}$	$\bar{x}$	$\bar{\sigma}$	$\bar{x}$	$\bar{\sigma}$
AIJ (2001)	1.07	0.18	0.94	0.13	1.07	0.04
Eurocode 4 (2004)	0.96	0.16	0.93	0.17	0.96	0.13
AS5100.6 (2004)	0.93	0.16	0.91	0.17	0.93	0.13
AISC (2005)	1.05	0.17	1.12	0.16	1.11	0.16
Proposed relationship	$\bar{x}$			$\bar{\sigma}$		
	0.99			0.14		

HSC, respectively. Furthermore, standard deviations of the ratios of N_{ue}/N_{uc} for the "AS5100.6 (2004)" model are 0.17. Thus, the "AS5100.6 (2004)" model is a more accurate prediction model for R-NSS-TC-HSC, R-HSS-TC-NSC, and R-HSS-TC-HSC experimental results.

5.2.2 Circular slender CFSTCs

Table 7 shows comparisons of the N_{ue}/N_{uc} ratios for the slender circular CFSTCs experimental results and available section capacity models in Table 4.

Figs. 10 to 16 show plots of the experimental ultimate load, N_{ue} for the slender C-NSS-TC-HSC, C-HSS-TC-NSC, and C-HSS-TC-HSC results versus the calculated ultimate load, N_{uc} for the available models and N_{ue}/N_{uc} ratios versus f'_c. Table 7 shows that the "Eurocode 4 (2004)", "AIJ (2001)", and "Eurocode 4 (2004)" models provide a better prediction with an average value of N_{ue}/N_{uc} ratios of 0.96, 0.94, and 0.96 compared with the other available models in Table 4 for the C-NSS-TC-HSC, C-HSS-TC-NSC, and C-HSS-TC-HSC, respectively. Furthermore, standard

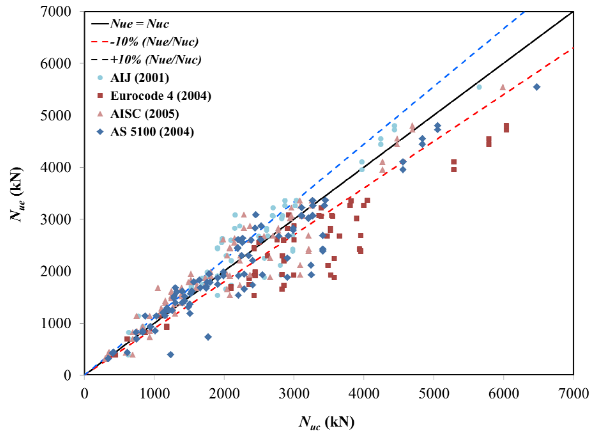

Fig. 10 Comparison of experimental results with predicted results by the existing models for slender C-NSS-TC-HSC

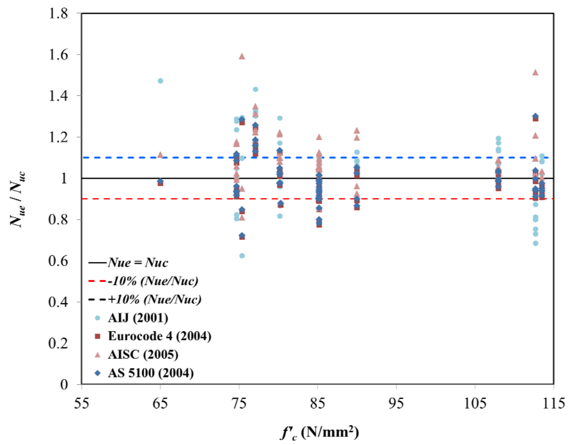

Fig. 11 Ratio experimental results/predicted results versus concrete strength for slender C-NSS-TC-HSC

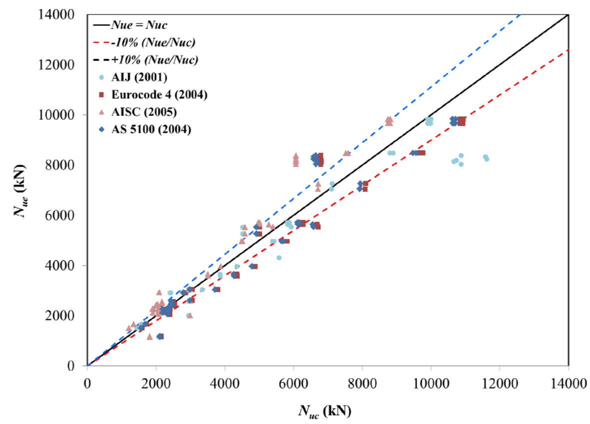

Fig. 12 Comparison of experimental results with predicted results by the existing models for slender C-HSS-TC-NSC

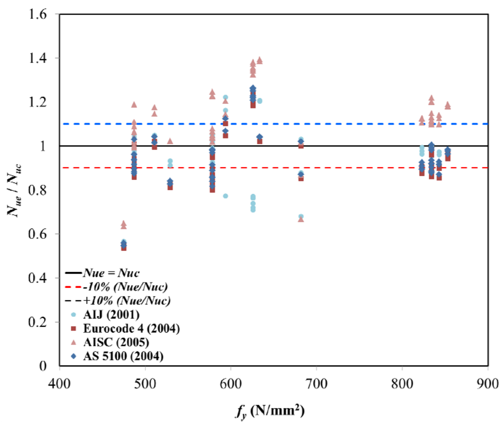

Fig. 13 Ratio experimental results/predicted results versus steel yielding strength for slender C-HSS-TC-NSC

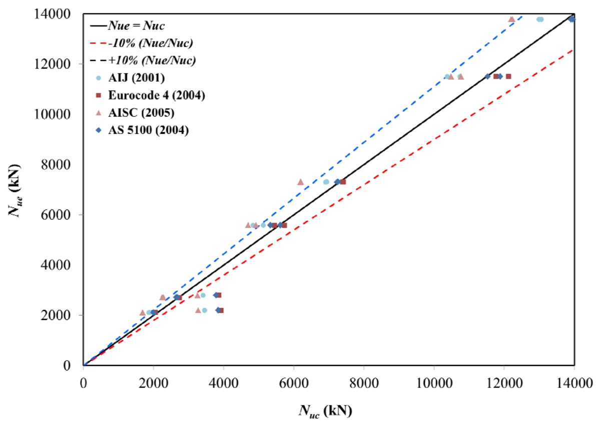

Fig. 14 Comparison of experimental results with predicted results by the existing models for slender C-HSS-TC-HSC

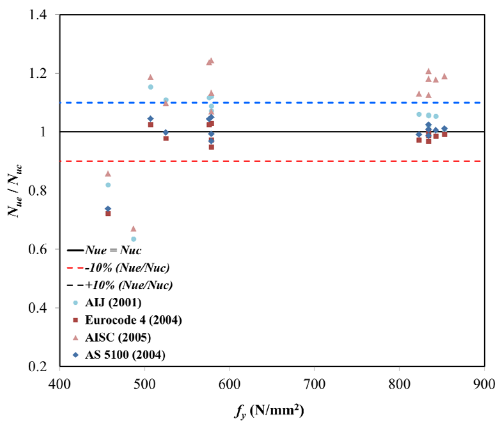

Fig. 15 Ratio experimental results/predicted results versus steel yielding strength for slender C-HSS-TC-HSC

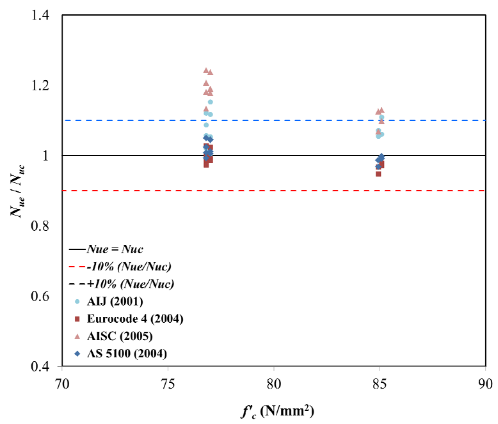

Fig. 16 Ratio experimental results/predicted results versus concrete strength for slender C-HSS-TC-HSC

deviations of the ratios of N_{ue}/N_{uc} for the "Eurocode 4 (2004)", "AIJ (2001)", and "Eurocode 4 (2004)" models are 0.16, 0.13, and 0.13 for the C-NSS-TC-HSC, C-HSS-TC-NSC, and C-HSS-TC-HSC, respectively. Thus, the "Eurocode 4 (2004)" model is a more accurate prediction model for C-NSS-TC-HSC, C-HSS-TC-NSC, and C-HSS-TC-HSC experimental results.

6. Proposed relationships for ultimate buckling capacity

The following conditions are considered in the new proposals for predicting the ultimate buckling capacity of rectangular and circular CFSTCs: (a) The essential modifications on the slenderness reduction factor based on the modified formula of section capacity should undertaken; (b) The equations should represent the experimental data as accurately as possible; (c) The mathematical form should be as simple as possible and applicable for any analysis; and (d) The equations are similar to existing ones so that engineers can readily make use of them in the practice of engineering design. Assimilating all the desirable conditions above and the best predicted models in section 5 for slender rectangular and circular CFSTCs, a new design relationship will be developed on the basis of the "AS5100.6 (2004)" model for rectangular CFSTCs and the "Sakino *et al*. (2004)" model as a simple model for circular CFSTCs. The details of the proposed relationship for rectangular CFSTCs are illustrated as Eqs. (3) to (10). Eqs. (3) to (10) have the following limitations as: $250 \leq f_y$ (N/m^2) ≤ 850, $20 \leq f'_c$ (N/mm^2) ≤ 130, and $19 \leq \lambda_e \leq 117$.

$$N_{uc} = \alpha_c N_{us} \leq N_{us} \tag{3}$$

$$N_{us} = A_s f_y + 0.87 A_c f'_c \tag{4}$$

$$\alpha_c = \xi \left[1 - \sqrt{1 - \left(\frac{90}{\xi \lambda} \right)^2} \right] \tag{5}$$

$$\xi = \frac{\left(\frac{\lambda}{90}\right)^2 + 1 + \eta_{\text{mod}}}{2\left(\frac{\lambda}{90}\right)^2} \tag{6}$$

$$\lambda = \lambda_\eta + \alpha_{a,\text{mod}}\,\alpha_b \tag{7}$$

$$\eta_{\text{mod}} = 0.00372(\lambda_\eta - 13.0) \geq 0 \tag{8}$$

$$\lambda_\eta = 90\,\lambda_r \tag{9}$$

$$\alpha_{a,\text{mod}} = \frac{2100\left(\lambda_\eta - 13.0\right)}{\lambda_\eta^2 - 15.3\,\lambda_\eta + 2050} \tag{10}$$

where N_{us} is the nominal section capacity which is proposed Eq. (1) in Sction 5, α_c is the compression member slenderness reduction factor, A_c is the area of the concrete cross section, A_s is the area of the steel tube cross section, f_y is the tensile yield stress of the steel tubes, f'_c is the compressive strength of the concrete, λ_η is the modified member slenderness, λ_r is the relative slenderness, and α_b is the appropriate section constant give in Table 10.3.3(A) or Table 10.3.3(B), AS5100.6 (2004).

Eqs. (3) to (10) are proposed based on the "AS5100.6 (2004)" model with empirical corrections and the regression analyses on the existing experimental data. The effective parameters are selected based on the regression analyses for modifying in the "AS5100.6 (2004)" model which are α_a and η. Fig. 17 shows plots of the N_{ue} versus N_{uc} for the proposed rectangular CFSTCs model and N_{ue}/N_{uc} ratios versus f'_c and f_y. As shown in Table 6, the proposed relationship for rectangular CFSTCs provides better prediction with an average value and standard deviation of N_{ue}/N_{uc} ratio of 0.97 and 0.14, respectively in comparison with the "AS5100.6 (2004)" model. Therefore, the proposed model in this study can be used to calculate the ultimate buckling capacity of normal and high-strength rectangular CFSTCs.

The details of the proposed relationship for circular CFSTCs are presented in Eqs. (11) to (16). Eqs. (11) to (16) have the limitations as: $20 \leq f_y$ (N/m^2) ≤ 860, $20 \leq f'_c$ (N/mm^2) ≤ 120, and $20 \leq \lambda_e \leq 195$.

$$N_u = A_s\sigma_{sz,\text{mod}} + A_c\sigma_{ccB,\text{mod}} \tag{11}$$

$$\sigma_{ccB,\text{mod}} = \gamma_U f'_c + 3.57\sigma_r \tag{12}$$

$$\gamma_U = 1.67\,D_c^{-0.112} \tag{13}$$

$$\sigma_r = -\frac{2t}{D-2t}\sigma_{s\theta} \tag{14}$$

$$\sigma_{s\theta} = -0.19\,f_y \tag{15}$$

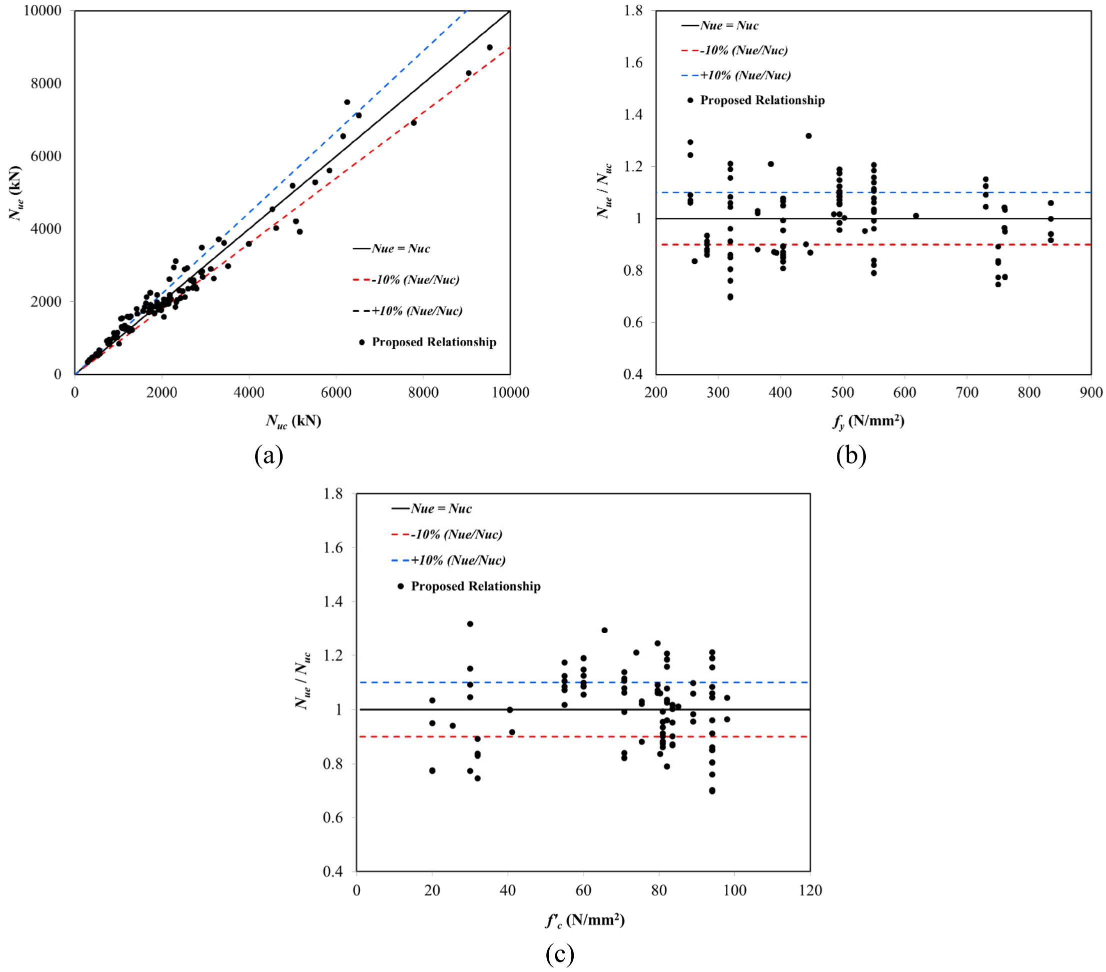

Fig. 17 Comparison of experimental results with predicted results by proposed relationship for slender rectangular CFSTCs

$$\sigma_{sz,\text{mod}} = 0.84\, f_y \tag{16}$$

where A_c is the area of the concrete cross section, A_s is the area of the steel tube cross section, σ_{ccB} is the strength of the confined concrete which considered proposed Eq. (2) in Section 5, σ_r is the confining stress, $\sigma_{s\Theta}$, $\sigma_{sz,mod}$ is the stress of the steel tube at the ultimate load, γ_U is the strength reduction factor for concrete, D is the diameter of the circular steel tube, D_c is the diameter of the concrete core, t is the wall thickness of the steel tube, f_y is the tensile yield stress of the steel tubes, and f'_c is the compressive strength of the concrete.

Eqs. (11) to (16) are developed on the basis of the "Sakino *et al*. (2004)" model with empirical corrections and the regression analyses on the existing experimental data. The effective parameter is selected based on the regression analyses for modifying in the "Sakino *et al*. (2004)" model which is σ_{sz}. Fig. 18 shows plots of the N_{ue} versus N_{uc} for the proposed circular CFSTCs model and N_{ue}/N_{uc} ratios versus f'_c and f_y. The proposed relationship for circular CFSTCs provides a better

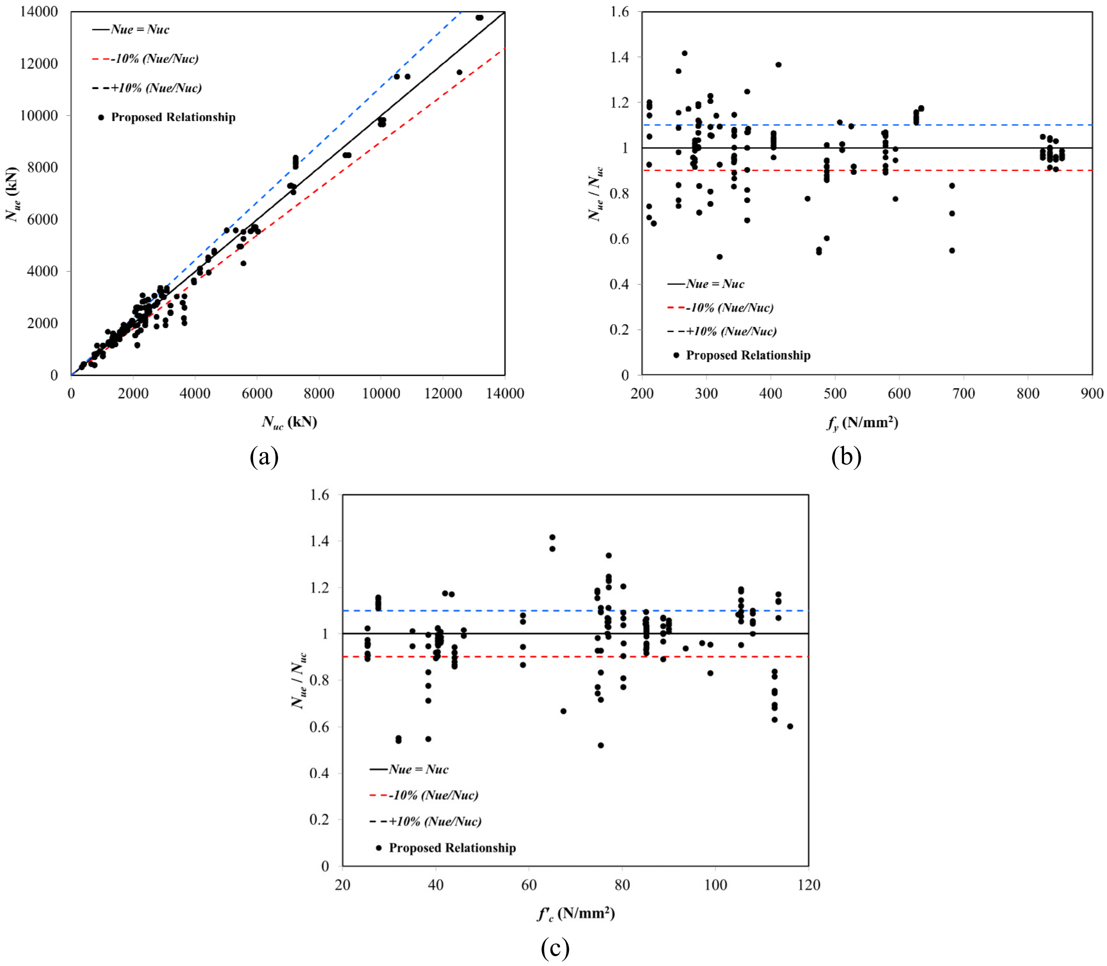

Fig. 18 Comparison of experimental results with predicted results by proposed relationship for slender circular CFSTCs

prediction with an average value and standard deviation of N_{ue}/N_{uc} ratio of 0.99 and 0.14, respectively in comparison with the "Sakino *et al*. (2004)" model, as shown in Table 7. Hence, the proposed method in this paper can be used to calculate the ultimate buckling capacity of normal and high-strength circular CFSTCs.

7. Discussion

The determination of section capacity and proposing a slenderness reduction factor to determine the overall buckling resistance for rectangular and circular CFSTCs have been done in Sections 5 and 6. All codes have provided some limitations on material strengths and section slenderness for design purposes. However, many tests have been conducted to date beyond those limitations, which makes it possible to check the potential of relaxing those limitations. The following sections will discuss the presented results in Sections 5 and 6.

7.1 Rectangular CFSTCs

The available models for rectangular CFSTCs showed different predictions when they are compared with each of the experimental databases (i.e., R-NSS-TC-HSC, R-HSS-TC-NSC, and R-HSS-TC-HSC), as illustrated in Figs. 1 and 3-9. The models in Table 3 are divided in two categories as conservative and unconservative models. The section capacity "AS (AS4100 2012, AS3600 2001), ACI (2005), and Eurocode 4 (2004)" models are conservative. Also, ultimate buckling capacity "AS5100.6 (2004)" model is conservative based on the calculated differences between N_{ue} and N_{uc}, respectively. The proposed relationships covered the section capacity and ultimate buckling capacity predictions of all three different short and slender R-NSS-TC-HSC, R-HSS-TC-NSC, and R-HSS-TC-HSC results.

7.2 Circular CFSTCs

The available models for circular CFSTCs showed different predictions when they are compared with each of the experimental databases (i.e., C-NSS-TC-HSC, C-HSS-TC-NSC, and C-HSS-TC-HSC), as illustrated in Figs. 2 and 10-16. The models in Table 4 are divided in two categories as conservative and unconservative models. The section capacity "AS (AS4100 2012, AS3600 2001), ACI (2005)" models are conservative. Also, ultimate buckling capacity "Eurocode 4 (2004) and AS5100.6 (2004)" models are conservative based on the calculated differences between N_{ue} and N_{uc}, respectively. The proposed relationships covered the section capacity and ultimate buckling capacity predictions of all three different short and slender C-NSS-TC-HSC, C-HSS-TC-NSC, and C-HSS-TC-HSC results.

8. Conclusions

In this paper simplified relationships have been developed to predict the section capacity and ultimate buckling capacity of normal and high-strength rectangular and circular CFSTCs subjected to concentric loading. The proposed relationships are developed based on a comprehensive study of available prediction models and collected experimental results. Eight existing design codes for rectangular CFSTCs and seven design codes for circular CFSTCs are also compared with the test results. The following conclusions can be made with the present scope of investigation:

(1) The results presented in this study are useful for providing a more accurate prediction of the section capacity and ultimate buckling capacity of normal and high-strength rectangular and circular CFSTCs and also will assist available codes of practice for the possible revision of their models for the use of high-strength CFSTCs in future.
(2) The "AS (AS4100 2012, AS3600 2001), ACI (2005), and Eurocode 4 (2004)" section capacity models were shown to provide a more accurate prediction model for short rectangular and circular CFSTCs experimental results.
(3) The "AS5100.6 (2004)" and "Eurocode 4 (2004)" ultimate buckling capacity models were shown to provide a more accurate prediction model for slender rectangular and circular CFSTCs experimental results, respectively.
(4) The ultimate buckling capacity proposed relationships for slender rectangular and circular CFSTCs are based on the "AS5100.6 (2004)" and "Sakino *et al.* (2004)" models with empirical corrections, respectively.

(5) The proposed relationships that are based on comprehensive analyses provide a direct and efficient representation of section capacity and ultimate buckling capacity of normal and high-strength rectangular and circular CFSTCs.

Acknowledgments

The authors would like to acknowledge the Australian Research Council Discovery Projects Grants Scheme for their financial support of this project under DP120101944 titled "The behaviour and design of composite columns coupling the benefits of high-strength steel and high-strength concrete for large scale infrastructure".

References

American Concrete Institute (ACI) (2005), Building code requirements for structural concrete and commentary, ACI 318-05; Farmington Hills, MI, USA.

American Concrete Institute (ACI) (2008), Building code requirements for structural concrete and commentary, ACI 318-08; Farmington Hills, MI, USA.

American Institute of Steel Construction (ANSI/AISC 360-05) (2005), "Specification for structural steel buildings", Chicago, Illinois, USA.

American Institute of Steel Construction (ANSI/AISC 360-10) (2010), Specification for Structural Steel Buildings, An American National Standard.

Architectural Institute of Japan (AIJ) (2001), Recommendations for design and construction of concrete filled steel tubular structures, Japan. [In Japanese]

Aslani, F., Uy, B., Tao, Z. and Mashiri, F. (2015), "Behaviour and design of composite columns incorporating compact high-strength steel plates", *J. Constr. Steel Res.*, **107**, 94-110.

CECS 28:90 (1992), Specification for design and construction of concrete-filled steel tubular structures, China Planning Press; Beijing, China. [In Chinese]

DBJ 13-51-2003 (2003), Technical specification for concrete-fi lled steel tubular structures, The Construction Department of Fujian Province; Fuzhou, China. [In Chinese]

De Oliveira, W.L.A., De Nardin, S., De Cresce, A.L.H. and El Debs, M.K. (2009), "Influence of concrete strength and length/diameter on the axial capacity of CFT columns", *J. Constr. Steel Res.*, **65**(12), 2103-2110.

Eurocode 4 (2004), Design of composite steel and concrete structures, Part1.1, General rules and rules for Building, BS EN 1994-1-1; British Standards Institution, London, UK.

Fujimoto, T., Nishiyama, I., Mukai, A. and Baba, T. (1995), "Test results of eccentrically loaded short columns–square CFT columns", *Proceedings of the Second Joint Technical Coordinating Committee Meeting on Composite and Hybrid Structures*, Honolulu, HI, USA, June.

Gho, W.M. and Liu, D.L. (2004), "Flexural behaviour of high-strength rectangular concrete-filled steel hollow sections", *J. Constr. Steel Res.*, **60**(11), 1681-1696.

GJB 4142-2000 (2001), Technical specifications for early-strength model composite structure used for navy port emergency repair in wartime, General Logistics Department of People's Liberation Army. [In Chinese]

Han, L.H., Liu, W. and Yang, Y.F. (2008), "Design calculations on concrete-filled thin-walled steel tubes subjected to axially local compression", *Proceedings of Tubular Structures XII*, Shanghai, China, October, pp. 85-91.

Hernández-Figueirido, D., Romero, M.L., Bonet, J.L. and Montalvá, J.M. (2012), "Ultimate capacity of rectangular concrete-filled steel tubular columns under unequal load eccentricities", *J. Constr. Steel Res.*, **68**(1), 107-117.

Hong Kong Buildings Department (2005), Code of practice for the structural use of steel.
Johansson, M. (2002), "The efficiency of passive confinement in CFT columns", *Steel Compos. Struct., Int. J.*, **2**(5), 379-396.
Johansson, M. and Gylltoft, K. (2001), "Structural behavior of slender circular steel-concrete composite columns under various means of load application", *Steel Compos. Struct., Int. J.*, **1**(4), 393-410.
Kilpatrick, A.E. and Rangan, B.V. (1999a), "Tests on high-strength concrete-filled steel tubular columns", *ACI Struct. J.*, **96**(2), 268-274.
Kilpatrick, A.E. and Rangan, B.V. (1999b), "Influence of interfacial shear transfer on behavior of concrete-filled steel tubular columns", *ACI Struct. J.*, **96**(4), 642-648.
Lam, D. and Gardner, L. (2008), "Structural design of stainless steel concrete filled columns", *J. Constr. Steel Res.*, **64**(11), 1275-1282.
Liew, J.Y.R. and Xiong, D.X. (2010), "Ultra-high-strength concrete filled columns for high rise buildings", *Proceedings of the 4th International Conference on Steel & Composite Structures*, (Keynote Lecture), Sydney, Australia, July, pp. 80-91.
Liew, J.Y.R and Xiong, D.X. (2012), "Ultra-high-strength concrete filled composite columns for multi-storey building construction", *Adv. Struct. Eng.*, **15**(9), 1487-1503.
Liew, J.Y.R., Chia, K.S., Kazi, M.A.S. and Xiong, D.X. (2008), "Innovation in Composite Construction—Towards the Extreme of High-strength and Lightweight", *Proceeding of the Fifth International Conference on Coupled Instabilities in Metal Structures*, (K. Rasmussen and T. Wilkinson Ed.), Mansonic Centre, Sydney, Australia, June, pp. 19-33.
Liu, D.L. (2004), "Behaviour of high-strength rectangular concrete-filled steel hollow section columns under eccentric loading," *Thin-Wall. Struct.*, **42**(12), 1631-1644.
Liu, D.L. (2005), "Tests on high-strength rectangular concrete-filled steel hollow section stub columns", *J. Constr. Steel Res.*, **61**(7), 902-911.
Liu, D.L. (2006), "Behaviour of eccentrically loaded high-strength rectangular concrete-filled steel tubular columns", *J. Constr. Steel Res.*, **62**(8), 839-846.
Liu, D., Gho, W.M. and Yuan, J. (2003), "Ultimate capacity of high-strength rectangular concrete-filled steel hollow section stub columns", *J. Constr. Steel Res.*, **59**(12), 1499-1515.
Lu, Z.H. and Zhao, Y.G. (2009), "A new design equation developed from Eurocode 4-2004 for concrete filled steel tubes", *Proceedings of the Sixth International Conference on Behavior of Steel Structures in Seismic Areas* (*STESSA 2009*), Philadelphia, PA, USA, August.
Melcher, J.J. and Karmazinova, M. (2004), "The analysis of composite steel-and concrete compression members with high-strength concrete", *Proceedings of SSRC Annual Technical Session*, pp. 223-237.
Mursi, M. and Uy, B. (2003), "Strength of concrete filled steel box columns incorporating interaction buckling", *J. Struct. Eng.-ASCE*, **129**(5), 626-639.
Mursi, M. and Uy, B. (2004), "Strength of slender concrete filled high-strength steel box columns", *J. Constr. Steel Res.*, **6**(12), 1825-1848.
Mursi, M. and Uy, B. (2006a), "Behaviour and design of fabricated high-strength steel columns subjected to biaxial bending, Part 1: Experiments", *Int. J. Adv. Steel Constr.*, Hong Kong Institute of Steel Construction, **2**(4), 286-315.
Mursi, M. and Uy, B. (2006b), "Behaviour and design of fabricated high-strength steel columns subjected to biaxial bending, Part 2: Analysis and design codes", *Int. J. Adv. Steel Constr.*, Hong Kong Institute of Steel Construction, **2**(4), 316-354.
National Standard of the People's Republic of China (GB50010-2002) (2002), Code for design of concrete structure, China Communications Press; Beijing, China. [In Chinese]
National Standard of the People's Republic of China (GB50017-2003) (2003), Code for design of steel structures, China Planning Press; Beijing, China. [In Chinese]
Packer, J.A. and Henderson, J.E. (2003), "Hollow structural section connections and trusses—A design guide", Canadian Institute of Steel Construction (CISC); Toronto, Canada.
Portolés, J.M., Romero, M.L., Filippou, F.C. and Bonet, J.L. (2011), "Simulation and design recommendations of eccentrically loaded slender concrete-filled tubular columns", *Eng. Struct.*, **33**,

1576-1593.
Rangan, B.V. and Joyce, M. (1992), “Strength of eccentrically loaded slender steel tubular columns filled with high-strength concrete”, *ACI Struct. J.*, **89**(6), 676-681.
Sakino, K., Nakahara, H., Morino, S. and Nishiyama, I. (2004), “Behavior of centrally loaded concrete-filled steel-tube short columns”, *J. Struct. Eng.-ASCE*, **130**(2), 180-188.
Sen, H.K. (1969), “Triaxial effects in concrete-filled tubular steel columns”, Ph.D. Thesis; University of London, England, UK.
Standards Association of Australia (2014a), AS/NZS 5100: Part 6-2014, Bridge Structures: Steel and Composite Structures, Sydney, Australia. [In Preparation]
Standards Association of Australia (2014b), AS/NZS 2327-2014: Composite Structures, Sydney, Australia. [In Preparation]
Standards Australia (AS3600-2001) (2001), Australian Standard: Concrete Structures.
Standards Australia (AS5100.6-2004) (2004), Bridge design, Part 6: Steel and composite construction, Sydney, Australia.
Standards Australia (AS3600-2009) (2009), Australian Standard: Concrete Structures.
Standards Australia (AS4100-1998) (2012), Amdt1-2012: Australian Standard: Steel structures.
Tao, Z., Uy, B., Han, L.H. and He, S.H. (2008), “Design of concrete-filled steel tubular members according to the Australian Standard AS 5100 model and calibration”, *Aust. J. Struct. Eng.*, **8**(3), 197-214.
Uy, B. (1999), “Axial compressive strength of steel and composite columns fabricated with high-strength steel plate”, *Proceedings of the Second International Conference on Advances in Steel Structures*, Hong Kong, December, pp. 421-428.
Uy, B. (2000), “Strength of short concrete filled steel box columns incorporating local buckling”, *J. Struct. Eng.-ASCE*, **126**(3), 341-352.
Uy, B. (2001a), “Axial compressive strength of short steel and composite columns fabricated with high-strength steel plate”, *Steel Compos. Struct., Int. J.*, **1**(2), 113-134.
Uy, B. (2001b), “Strength of short concrete filled high-strength steel box columns”, *J. Constr. Steel Res.*, **57**(2), 113-134.
Uy, B., Mursi, M. and Tan, A. (2002), “Strength of slender composite columns fabricated with high-strength structural steel”, *Proceedings of ICASS’02 Third International Conference on Advances in Steel Structures*, Hong Kong, December, pp. 575-582.
Uy, B., Khan, M., Tao, Z. and Mashiri, F. (2013), “Behaviour and design of high-strength steel concrete filled columns”, *Proceedings of the 2013 World Congress on Advances in Structural Engineering and Mechanics* (*ASEM13*), Jeju, Korea, September, pp. 150-167.
Varma, A.H., Ricles, J.M., Sause, R. and Lu, L.W. (2002a), “Experimental behavior of high-strength square concrete-filled steel tube beam-columns”, *J. Struct. Eng.-ASCE*, **128**(3), 309-318.
Varma, A.H., Ricles, J.M., Sause, R. and Lu, L.W. (2002b), “Seismic behavior and modeling of high-strength composite concrete-filled steel tube (CFT) beam-columns”, *J. Constr. Steel Res.*, **58**(5-8), 725-758.
Varma, A.H., Ricles, J.M., Sause, R. and Lu, L.W. (2004), “Seismic behavior and design of high-strength square concrete-filled steel tube beam columns”, *J. Struct. Eng.-ASCE*, **130**(2), 169-179.
Yi, S.-T., Yang, E.-I. and Choi, J.-Ch. (2006), “Effect of specimen sizes, specimen shapes, and placement directions on compressive strength of concrete”, *Nucl. Eng. Des.*, **235**, 115-127.
Yu, X.M. and Chen, B.C. (2011), “A statistical method for predicting the axial load capacity of concrete filled steel tubular columns”, *Int. J. Civil Env. Eng.*, **11**(2), 20-39.
Yu, Q., Tao, Z. and Wu, Y.X. (2008), “Experimental behaviour of high performance concrete-filled steel tubular columns”, *Thin-Wall. Struct.*, **46**(4), 362-370.

CC